

Preparation of highly emissive, thermally stable, UV-cured polysilsesquioxane/ZnO nanoparticle composites

Hyeonyeol Jeon,^{1,2} Albert Sung Soo Lee,¹ Hyun-Ji Kim,¹ So-Hye Cho,^{1,2}
Kyung-Youl Baek,^{1,2} Seung Sang Hwang^{1,2}

¹Materials Architecturing Research Center, Korea Institute of Science and Technology, Hwarangno 14-gil 5, Seong-Buk Gu, Seoul 136-791, Republic of Korea

²Nanomaterials Science and Engineering, University of Science and Technology, 217 Gajungro, 176 Gajung-dong, Yuseong-Gu Daejeon, Korea 305-333

H. Jeon and A. S. Lee contributed equally to this work.

Correspondence to: S.S. Hwang (E-mail: sshwang@kist.re.kr)

ABSTRACT: A high molecular weight polysilsesquioxane (LPMSQ)/ZnO nanocomposite was prepared by blending a methacryl-substituted polysilsesquioxane and PMMA-coated ZnO nanoparticle (NP) followed by UV-curing process. These LPMSQ/ZnO nanocomposites gave high thermal and mechanical stabilities originated from the rigid ladder structured siloxane backbone of LPMSQ. The polysilsesquioxane and surface-modified ZnO nanoparticles showed excellent compatibility between MMA groups in LPMSQ- and PMMA-capped ZnO nanoparticles to give well-dispersed LPMSQ/ZnO nanocomposites. Mechanically pliant and flexible free standing films were obtained, and the photo and optical properties of these hybrid nanocomposites were examined. The high photoluminescent properties were maintained even after severe thermal treatments exceeding 400°C. © 2015 Wiley Periodicals, Inc. *J. Appl. Polym. Sci.* 2015, 132, 42333.

KEYWORDS: blends; composites; nanoparticles; nanowires and nanocrystals; optical properties; thermal properties

Received 20 January 2015; accepted 7 April 2015

DOI: 10.1002/app.42333

INTRODUCTION

Zinc oxide (ZnO) nanoparticles have received considerable attention as polymer nanocomposites due to their wide range of applications such as energy harvesting materials, electrical devices, optoelectronic materials for displays, drug delivery, and chemical, bio-labelling, gas sensors.¹⁻⁶ These applications are possible due to the transparent and luminescent properties of ZnO in nanostructured form. ZnO nanoparticles are optimum materials for short-wavelength optoelectric applications owing to their wide band gap (3.37eV) and large exciton binding energy at room temperature. The origin of the visible luminescent nature of ZnO is still controversial among researchers. However, the most acceptable explanation is the oxygen vacancies (or defects), as N-type semiconducting properties have been shown, as carriers of electrons of oxygen vacancy which act as electron donor move to conduction band when external energy is applied.⁷⁻⁹

Arising from these properties, ZnO has been reported to have strong photoluminescent (PL) properties even in combination

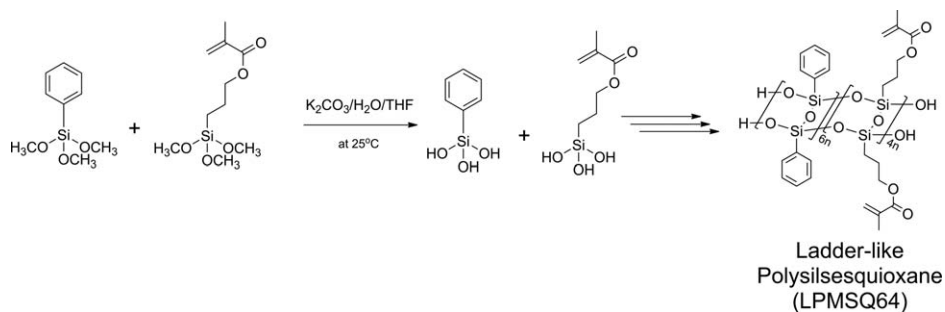
with various polymers. In addition to the photoluminescent properties, tuning of the surface properties with regards to surface passivation via surfactant and capping agents using polymers have been investigated in detail.¹⁰⁻¹³

The choice of surfactant depends on the nanoparticle's core, size, and solvents. Hydrocarbon-based ligands allow for high solubility in organic solvents such as hexane, toluene, and chloroform, while polar or aqueous ligands imbue dispersibility under aqueous conditions. In aqueous solutions, strongly charged ligand molecules, containing oleic acid, oleyl amine, carboxylic acid, or sulphonic groups, are found to stabilize the particles for longer periods of time and at more elevated salt concentrations.^{14,15} In addition, NPs are also affected by capping polymers as various reasons for stabilization to prevent aggregation at interfacial interaction between nanoparticles and polymers.

However, for applications of nanoparticles within a polymer matrix, there can bring about various problems.^{16,17} One representative drawback is the thermal decomposition temperature

Additional Supporting Information may be found in the online version of this article.

© 2015 Wiley Periodicals, Inc.



Scheme 1. Synthesis of ladder-like poly(phenyl-co-methacryloxypropyl)silsesquioxane (LPMSQ).

that originated from most organic polymers. One of the trends between several established methods is that overcome these shortcomings is hybridization with organic–inorganic materials. As aforementioned, there has been existed that surface modification to stabilize the nanoparticle and increase of compatibility with polymers by means of using silanes such as TEOS, APTES. However, these silane capping agents are structurally unstable which allows for chemical degradation and photooxidation.^{18,19} On the other hand, in case of nanocomposites with representative organic polymers such as PS, PMMA, PVP, PEG, PEO that commonly are confronted with high thermal decomposition at elevated temperatures which limit their applications in optoelectronic devices, especially regarding long-term stability.

There are many research works related to applications of optoelectric, energy harvesting, transparent display, and so on.^{1–6} Also, these aforementioned polymers are undeniably appropriate for these purposes. However, their most demerits are remarkable thermal stability. Especially for the energy harvesting and transparent display substrate's low thermal resistance are directly related to durability of function. Matsuyama *et al.* reported the composite of transparent and emission tunable ZnO/PMMA hybrids.²⁰ However, nowadays requirements of enhanced function of thermal properties, dimensional stability, transparency, flexibility related to durability are critical to improve upon device performance.

Polysilsesquioxanes are unique class of inorganic–organic hybrid materials in which the chemical formula is $[\text{RSiO}_{1.5}]_n$. Equipped with a $-\text{R}$ organic functional group, polysilsesquioxanes exhibit high thermal stability, excellent mechanical properties, and optical transparency. There are three structural classes of polysilsesquioxanes: random branched, cage, and ladder-like type. While all of these structures have multiple uses, fully condensed, ladder-like, thermoplastic polysilsesquioxanes are of special interest in fabricating polymer nanocomposites, due to its high solubility, high molecular weight, and superior thermal properties, which can be attributed to the lack of uncondensed silanol groups. These lacks of uncondensed silanol groups vastly simplify the processing as well as increase the thermal stability of the nanocomposite, while maintain organic polymer-like mechanical pliancy.

In this article, we report a new polymer–nanoparticle composite incorporating a UV-curable poly(phenyl-co-methacryl silsesquioxane) (LPMSQ) with methacryl moieties which are able to be photocured and compatible with the MMA group of ZnO surface. The photoluminescence and thermal properties of this novel polysilses-

quioxane with ZnO were fabricated and verified. We contend that these siloxane containing hybrid polymers can be thought to reinforce the disadvantages of poor thermal properties and durability compared to fully organic polymer based materials.

EXPERIMENTAL

Materials

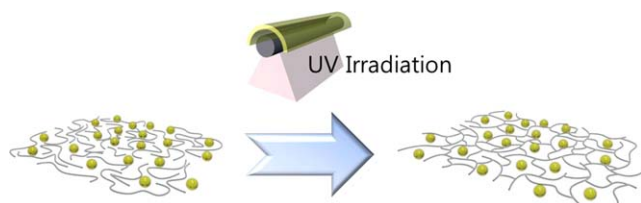
Zinc acetate dihydrate (Zinc $(\text{CH}_3\text{COO})_2 \cdot 2\text{H}_2\text{O}$, 99.999%, Sigma-Aldrich), lithium hydroxide monohydrate ($\text{LiOH} \cdot \text{H}_2\text{O}$, 98.0%, Sigma-Aldrich), and potassium carbonate (K_2CO_3 , 99.9%, Sam-chun) were used as received. 3-Methacryloxypropyltrimethoxysilane (TPM, 98.0%, Shin-Etsu) and phenyltrimethoxysilane (PTMS, 98.0%, Shin-Etsu) were vacuum distilled. Azobisisobutyronitrile (AIBN, 99.0%, Daejung chem.) was recrystallized with methanol and Methylmethacrylate (MMA, 99.0%, Sigma-Aldrich) was purified by vacuum distillation over calcium hydride (CaH_2 , Sigma-Aldrich). Ethyl alcohol anhydrous (99.9%, Daejung chem.) was used as solvent without further purification. Photoinitiator (1-hydroxycyclohexyl phenyl ketone, Irgacure 184, BASF) was used as received.

Synthesis of Ladder-Like Polysilsesquioxane (LPMSQ)

The polymer used in this study was UV-curable polysilsesquioxane synthesized by our group (Scheme 1).^{21–23} In a 100-mL round-bottomed flask, deionized water (2.4 g, 0.133 mol), and potassium carbonate (K_2CO_3) (0.02 g, 0.145 mmol, Sam-chun) were charged and stirred for 10 min. Dry THF (4 g, 0.056 mol, J. T. Baker) was added and stirred for additional 30 min. Afterwards, methacryloxypropyltrimethoxysilane (16 mmol, 3.97 g) and phenyltrimethoxysilane (24 mmol, 4.76 g) monomer mixtures were added dropwise via syringe under nitrogen and the reaction kept for stirring at room temperature for 96 h. LPMSQ64 was prepared from mole-ratios of phenyl:methacryloxypropyl mole ratio of 6 : 4, named LPMSQ. After 96 h, the crude was divided into two phases as colorless and cloudy phases. Crude, viscous products were obtained by decantation of the colorless mixed solvent. The weight averaged molecular weight was 38,000 g/mol and PDI was 2.4.

Synthesis of Zinc Oxide Nanoparticle

All the glassware was dried in a drying oven for 4 h. Zinc acetate dihydrate and lithium hydroxide monohydrate were dissolved in 100 mL of ethanol and pre-stirred at room temperature to give completely dispersed solutions. After that, the vigorous stirring was conducted for 2 h at 70°C under argon atmosphere. Also, we controlled various amounts of the mole



Scheme 2. Casting and photo-curing of composite film. [Color figure can be viewed in the online issue, which is available at wileyonlinelibrary.com.]

ratio zinc acetate dihydrate and lithium hydroxide monohydrate at 1 : 0, 1 : 1, 1 : 1.5, and 1 : 4 to give tunable emission^{24–26} (Supporting Information Figures S1–S3). There exists the critical concentration of ratio between LiOH and zinc acetate to hydrolyze properly controlling the size-induced nucleation growth and agglomeration within particles except 1 : 0 mole ratio.^{20,27,28} Afterwards, TPM (3-(Trimethoxysilyl)propyl methacrylate) and deionized water (50 μL : 100 μL) were injected to precursor solution for surface modification. Further vigorous stirring were conducted for more 2 h. Then, purified MMA monomer and AIBN were added to give complete dispersed solution, to polymerize and cap the ZnO precursor for overnight under Ar atmosphere with 70°C vigorous stirring. All the ZnO nanoparticle used in this study which contains the mole ratio of MMA:AIBN was 40 mol : 0.244 mol as capping material. White precipitations were observed and purified by precipitation in ethanol to remove unreacted monomers and precursors using centrifugation of 3000 rpm several times. The polymerization was controlled as such the PMMA content sized at 60 wt %. All the composited samples used in each characterization had a ZnO nanoparticle size of 5 nm.

Preparation of Composite Film by Solution Casting

LPMSQ (with photoinitiator)/ZnO nanoparticle were mixed in THF with sonication under homogeneous and poured on the Teflon vessel. The contents of ZnO NPs were 1, 3, 5, 10, and 20 wt % with respect to LPMSQ as matrix, with 1 wt % photoinitiator Igracure 184 added with respect to the LPMSQ matrix. These samples were designated as ZSQ1, ZSQ3, ZSQ5, ZSQ10, and ZSQ20 corresponding to the ZnO NP loading percentage. The casted solution was kept in room temperature overnight and dried on the hot plate set at 80°C for complete evaporation of the residual solvent.

The prepared composite films were photo-cured under a 365 nm UV lamp irradiated with a total UV energy output of 3 J/cm². Transparent and flexible coin-shaped composite films were prepared through this simple procedure (Scheme 2).

Characterization

The photoluminescence were measured in air with JASCO FP-6500 FL spectrofluorometer. Transmission Electron Microscopy was conducted on a FEI Tecnai F20 instrument equipped with a 200 kV field emission gun. Samples for TEM analysis were prepared by dropping small aliquots of the ZnO solutions onto Cu grids with ultrathin carbon type-A, 400 mesh (TED PELLA). Thermal gravimetric analysis (TGA, TA instrument, Q50) were examined ranging from 30 to 800°C at heating rate of 10°C /

min under nitrogen atmosphere for thermal properties between nanoparticle- and siloxane-based polymer.

Characterization of ladder-like polysilsesquioxane (LPMSQ) was conducted on 400 MHz ¹H NMR (Bruker Ascend 400, 400 MHz) using CDCl₃ at 25°C. Fourier transform infrared spectroscopy (FT-IR) was examined with a Thermo Nicolet iS10 using solvent cast films on KBr pellet. The number average molecular weight (Mn) and molecular weight distributions (Mw/Mn) of the polymers were measured by JASCO PU-2080 plus SEC system equipped with a differential RI-2031 detector and a UV-2057 detector (250-nm detection wavelength) using THF as the mobile phase at 40°C and a flow rate of 1 mL/min. Calibration based on polystyrene standards was applied for determination of molecular weights and polydispersity of polymer. UV photocuring was conducted using Hithachi UV Cure System. TMA thermograms were obtained in film fiber mode of TMA 2940, Thermomechanical Analyzer, TA instrument at temperature range of 0–300°C with scan rate of 10°C/min. Nanoindentation measurements were conducted on a Hysitron Inc. TriboIndenter[®] equipped with a Berkovich diamond tip. Measurements of elastic modulus were performed as continuous stiffness measurement technique. With this technique, each indent gives elastic modulus as a continuous function of the indenter's displacement into the samples. Ten indentations were performed on each sample. Loading was controlled such that the loading rate divided by the load was held constant at 0.5/s.

RESULTS AND DISCUSSION

Fabrication of Hybrid Nanocomposites

The ZnO NPs were synthesized with different sizes to observe their tunable PL emission^{20,24–28} as well as their compatibility with the silsesquioxane matrix. The polysilsesquioxane matrix used in this study had a phenyl : methacryloxypropyl mol ratio of 6 : 4. The phenyl moieties provided thermal stability and film robustness, and the methacryloxypropyl groups have a photocurable, as well as flexible function. These methacryloxypropyl groups also functioned to provide excellent compatibility between the PMMA-capped ZnO nanoparticles as well.^{21–23}

Furthermore, we carried out fabricating the hybrid nanocomposite film using the well-dispersed ZnO nanoparticle solutions blended with silsesquioxane in THF at a total solid content of 10 wt % at various ZnO emission induced by Zn(OAc)₂/LiOH ratio. (Figure 1) While ZnO capped with PMMA only was unable to form free standing films, the hybrid nanocomposite film containing LPMSQ was formed well with good flexibility. Also, the composite films were solution blended and well formed. Obtained composites films were also highly flexible, as the LPMSQ had high molecular weight and film robustness. Moreover, the hybrid composite films were highly transparent under day sunlight and displayed under ambient UV irradiation ($\lambda = 350$ nm). These composited films presented different PL emissions. These can be derived from different mole ratio of zinc acetate dehydrate and lithium hydroxide monohydrate. (see Figures S1–S3 in Supporting Information) Also, we observed that the wavelengths of PL spectra were changed to go through red shift. It means that the particle size was increased as LiOH decreasing related quantum confinement effect which is

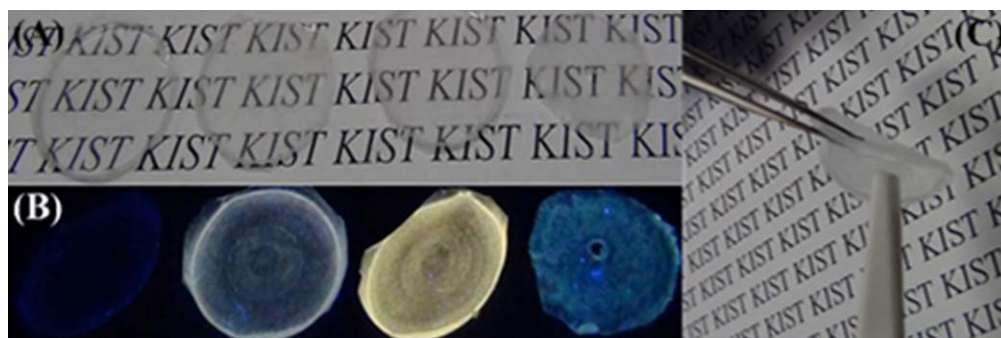


Figure 1. (A) Photographs of ZSQ10 composite films (B) under UV irradiation, (C) composite film showing good flexibility. [Color figure can be viewed in the online issue, which is available at wileyonlinelibrary.com.]

described later. However, for the samples containing only PMMA-capped ZnO without LPMSQ blending, free standing film formation was not observed, as these composite films were extremely brittle.

The photocuring process was monitored by FT-IR. As shown in Figure 2, the unsaturated C=C bonds at 1640 cm^{-1} attributed to the methacryloxypropyl groups of LPMSQ and TMS were completely disappeared after photocuring, as thus we were able to confirm that photo-curing occurred perfectly completely without any unreacted monomers under UV irradiation conditions of 3 J/cm^2 .

Figure 3 showed the PL intensities with increasing ZnO concentration of composites. It is interesting to note that no aggregation or quenching was observed. Generally, existing thin films prepared by many methods like spin casted, drop casted that show peak shifts attributed to the aggregation of the nanoparticles.^{23,29} However, in our blend and photocurable composite system, methacryl moiety of nanoparticle surface was found to be highly miscible with the pendant of siloxane-based polymer matrix, the dispersion can be maintained in the dispersed state, even after photocuring.

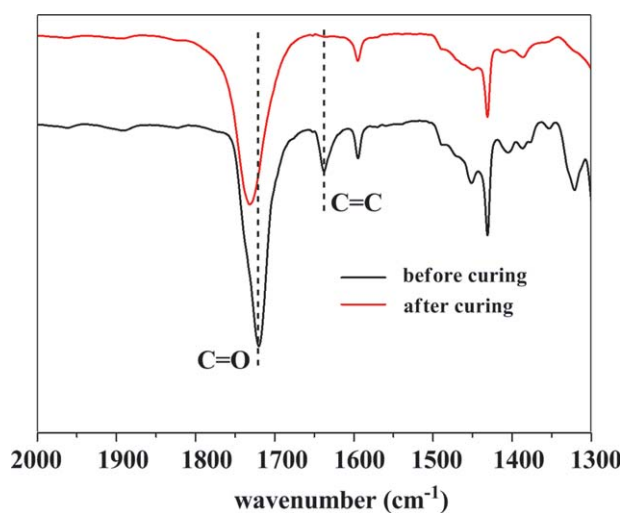


Figure 2. FT-IR spectrum of ZSQ film before and after UV-curing. [Color figure can be viewed in the online issue, which is available at wileyonlinelibrary.com.]

In Figure 4, we confirmed that ZnO nanoparticles ($\sim 5\text{ nm}$) were well dispersed within the LPMSQ polymer matrix without aggregation even at a concentration of 10 wt % loading. These dispersion states without aggregation are important in view of a blending system which could not be processed transparently which may affect to decrease the PL emission.

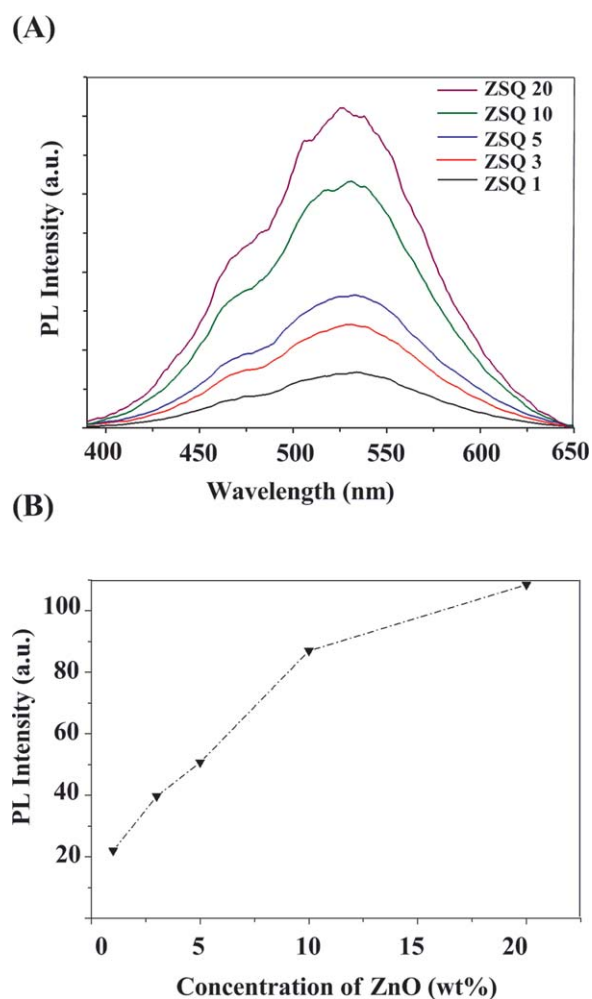


Figure 3. PL Spectra of spin casted film on the quartz plate with various contents of ZnO with LPMSQ, (A) PL spectra, (B) Max intensity value change. [Color figure can be viewed in the online issue, which is available at wileyonlinelibrary.com.]

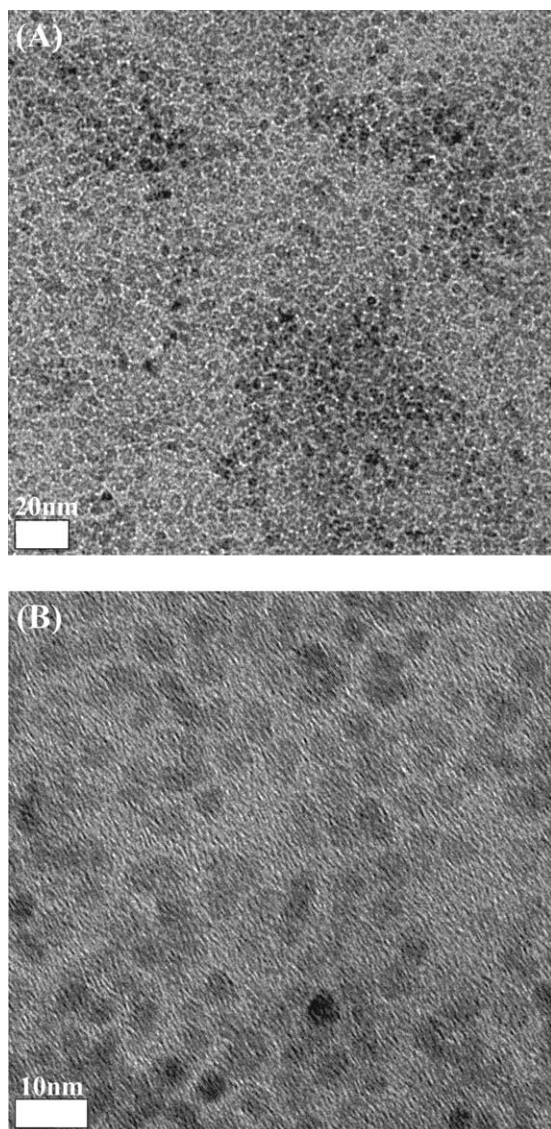


Figure 4. TEM Images of ZSQ10.

Thermal Properties of Composite Films

We examined thermal decomposition temperature of the composite films by means of TGA. The TGA result (Figure 5) of LPMSQ composite ZSQ20 exhibited excellent thermal stability in comparison with only PMMA capped 20 wt % of ZnO without blending with LPMSQ. ZnO capped with only PMMA composite begins to decompose below 200°C, which was attributed to the degradation of the surface –OH groups of the TPM silane, followed by degradation of the PMMA grafts around 300°C. While LPMSQ containing composite was stable up to 400°C although they have organic groups. LPMSQs are unique, in that there was no weight loss before thermal degradation of the organic functional groups. This excellent thermal stability derives from the fully condensed, rigid silsesquioxane backbone with no uncondensed silanol groups, which only reside on the polymer ends.^{30,31} This unique thermal stability imbues both excellent thermoplastic properties before photocuring which allows for facile blend, casting, and photocuring processing.

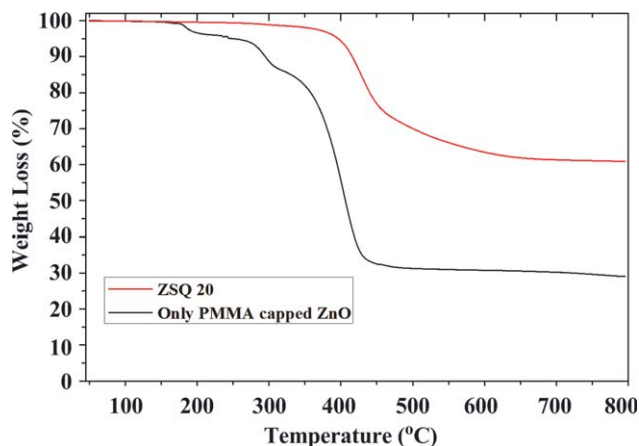


Figure 5. TGA curves of composite film. [Color figure can be viewed in the online issue, which is available at wileyonlinelibrary.com.]

Also, these thermally stable properties of hybrid composites can maintain the characteristics of organic-based NPs effectively.

The thermomechanical properties of polymer–nanoparticle composites are also of critical importance when considering device-level integration.^{32–34} Through thermomechanical analyses (TMA) of the free-standing ZSQ composite films before and after photo-curing, we were able to measure the coefficient of thermal expansion (CTE) values for the ZSQ composites with various ZnO NP contents. Figure 6(A) shows the TMA thermogram of LPMSQ before photocuring and after photocuring with various ZnO NP contents. Before photocuring, LPMSQ showed a glass transition at approximately 110°C, which was attributed to the organic functional composition of phenylmethacryloxypropyl groups, as high molecular weight polysilsesquioxanes conventionally do not show a glass transition derived from the rigid siloxane backbone. Below the glass transition temperature, the CTE of LPMSQ was found to be 126 ppm/K, while over the glass transition temperature, the CTE was 210 ppm/K. While these values were comparable compared to conventional organic polymers, with the incorporation of photocured ZnO NP surface coated with PMMA, these hybrid nanocomposites exhibited exceeding low CTE values. When ZnO NPs was loaded at 1 wt %, 5 wt %, and 10 wt %, the CTE value were reduced to 33.5 ppm/K, 31.3 ppm/K, and 30.1 ppm/K, respectively. Moreover, the TMA thermograms of the ZSQ showed no discernible transitions, which indicated that the nanosized ZnO NPs were well dispersed and the photocuring process complete.^{35–38} In addition, the nanoindentation results of UV-cured LPMSQ, as well of ZnO composites, were summarized in Figure 6(B) As shown, both the modulus and hardness values drastically increased with increasing ZnO content. It was noteworthy that the modulus values obtained for ZSQ5 and ZSQ10 were substantially higher than previously studied hybrid materials, with a high modulus of 9.4 GPa.³⁹ Both the TMA and nanoindentation results revealed that with ZnO nanoparticles, as structural support agents for the LPMSQ matrix, were extremely effective in forming a highly cross-linked network structure with robust thermomechanical properties, which are greatly promising properties for future application in optoelectronic devices.

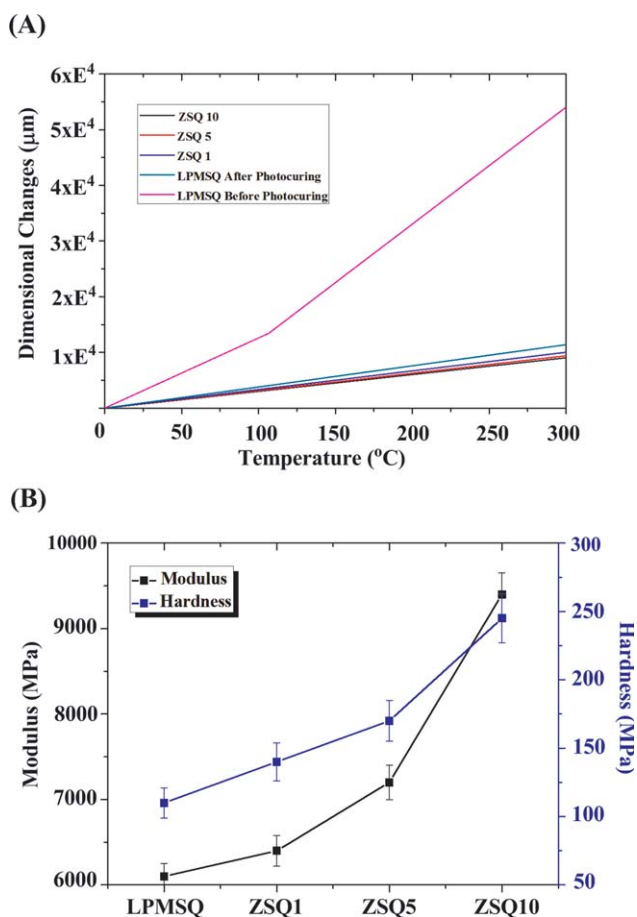


Figure 6. (A) TMA Thermograms of LPMSQ (B) Elastic properties of LPMSQ & photocured ZSQ series. [Color figure can be viewed in the online issue, which is available at wileyonlinelibrary.com.]

Figure 7 shows the stability of ZnO nanoparticles through PL intensity changes after thermal treatments at various temperatures. The ZnO [(a) 10 wt %, (b) 20 wt %] containing composite thin films were spin-coated on the quartz plates and heat treated under Argon atmosphere for 30 min to prevent oxida-

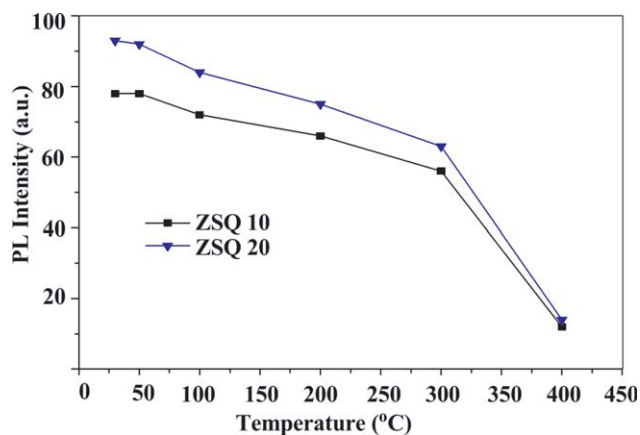


Figure 7. PL Intensity changes on the heat treatment under Ar atmosphere with various temperatures. [Color figure can be viewed in the online issue, which is available at wileyonlinelibrary.com.]

tion. After that, PL was measured promptly. Up to thermal treatments of 200°C, only a small decrease in PL intensity was observed. However, for thermal treatments exceeding 300°C, the PL intensity decreased drastically. These PL properties reduction tendencies caused by that organic pendant of siloxane-based polymers are unstable around 400°C and begun to degrade. However, the possible exists that within the polymer matrix, some aggregation of ZnO may form during severe thermal treatments considering the small size (5 nm) of the ZnO nanoparticle, as compared to a previous study which crosslinked submicron-sized ZnO-polyimide monomers *in situ* at over 200°C while maintaining high emissive behavior.⁴⁰ Notwithstanding these points, we were able to demonstrate extremely high durability even though heat treatment in high temperature. Based on these results, further studies from the point of view of thermomechanical properties related to energy harvesting are currently being investigated. Moreover, the ease in which a polymer–nanoparticle composite can be fabricated through solution-blending over *in situ* polymerization shows that our method may be applicable in a wide range of applications.

CONCLUSIONS

We successfully synthesized ZnO nanoparticles and fabricated a new class of hybrid ZnO NP/ poly(phenyl-co-methacryl)silsesquioxanes (LPMSQ) composites to generate free-standing films using a simple and versatile solvent casting and photocuring processes. The thermal properties of ZnO/LPMSQ composites were investigated by TGA and TMA, which showed thermal stability above 400°C and low CTE values (~30 ppm/K), while the PL intensities were shown to be maintained after thermal treatments exceeding 200°C. The effects of polymer matrix with proper nanosized NPs were discussed as possible next generation transparent and luminescent optoelectronic device applications.

ACKNOWLEDGMENTS

This work was supported by Nano-Convergence Foundation (www.nanotech2020.org) funded by the Ministry of Science, ICT and Future Planning (MSIP, Korea) & the Ministry of Trade, Industry and Energy (MOTIE, Korea) [R201400310], and partially supported by a grant from Materials Architecturing Research Center of Korea Institute of Science and Technology.

REFERENCES

- Aaronson, C. H.; Amekura, H.; Sato, Y.; Kishimoto, N. *J. Appl. Phys.* **2011**, *109*, 024506.
- Palanikumar, L.; Ramasamy, S.; Hariharan, G.; Balachandran, C. *Appl. Nanosci.* **2012**, *3*, 441.
- Qu, M.; Tu, H.; Amarante, M.; Song, Y. Q.; Zhu, S. S. *J. Appl. Polym. Sci.* **2014**, *131*, 40287.
- Bai, S.; Hu, J.; Li, D.; Luo, R.; Chen, A.; Liu, C. C. *J. Mater. Chem.* **2011**, *21*, 12288.
- Fan, Z.; Wang, D.; Chang, P. C.; Tseng, W. Y.; Lu, J. G. *Appl. Phys. Lett.* **2004**, *85*, 5923.

6. Tang, X.; Choo, E. S. G.; Li, L.; Ding, J.; Xue, J. *Chem. Mater.* **2010**, *22*, 3383.
7. Vanheusden, K.; Seager, C. H.; Warren, W. L.; Tallant, D. R.; Voigt, J. A. *Appl. Phys. Lett.* **1996**, *68*, 403.
8. Guo, L.; Yang, S. *Chem. Mater.* **2000**, *12*, 2268.
9. Guo, L.; Yang, S.; Yang, C.; Yu, P.; Wang, J.; Ge, W.; Wong, G. K. L. *Appl. Phys. Lett.* **2000**, *76*, 2901.
10. Thomas, S. P.; Mathew, E. J.; Marykutty, C. V. *J. Appl. Polym. Sci.* **2012**, *124*, 3099.
11. Zhang, J. J.; Gao, G.; Zhang, M.; Zhang, D.; Wang, C. L.; Zhao, D. C.; Liu, F. Q. *J. Colloid Interface Sci.* **2006**, *301*, 78.
12. Zhang, L.; Li, F.; Chen, Y.; Wang, X. *J. Lumin.* **2011**, *131*, 1701.
13. Sato, M.; Kawahara, Y.; Morito, S.; Yamaguchi, I.; Fujita, Y. *Eur. Polym. J.* **2012**, *48*, 1177.
14. Grubbs, R. B. *Polym. Rev.* **2007**, *47*, 197.
15. Braam, D.; Mölleken, A.; Prinz, G. M.; Notthoff, C.; Geller, M.; Lorke, A. *Phys. Rev. B.* **2013**, *88*, 125302.
16. Hammer, N. I.; Emrick, T.; Barnes, M. D. *Nanoscale Res. Lett.* **2007**, *2*, 282.
17. Sperling, R. A.; Parak, W. J. *Philos. Trans. R. Soc. A* **2010**, *368*, 1333.
18. Zhou, H.; Alves, H.; Hofmann, D. M.; Meyer, B. K.; Kaczmarczyk, G.; Hoffmann, A.; Thomsen, C. *Phys. Status Solid B* **2002**, *229*, 825.
19. Woo, J. Y.; Lee, J.; Han, C. S. *Nanotechnology* **2013**, *24*, 505714.
20. Matsuyama, K.; Mishima, K.; Kato, T.; Irie, K.; Mishima, K. *J. Colloid Interface Sci.* **2012**, *367*, 171.
21. Choi, S. S.; Lee, H. S.; Hwang, S. S.; Choi, D. H.; Baek, K. Y. *J. Mater. Chem.* **2010**, *20*, 9852.
22. Lee, A. S.; Choi, S. S.; Lee, H. S.; Jeon, H. Y.; Baek, K. Y.; Hwang, S. S. *J. Polym. Sci. Part A: Polym. Chem.* **2012**, *50*, 4563.
23. Zhang, J.; Gao, G.; Liu, F. J. *J. Appl. Polym. Sci.* **2013**, *128*, 2162.
24. Xiong, H. M.; Ma, R. Z.; Wang, S. F.; Xia, Y. Y. *J. Mater. Chem.* **2011**, *21*, 3178.
25. Fu, Y. S.; Du, X. W.; Kulinich, S. A.; Qiu, J. S.; Qin, W. J.; Li, R.; Sun, J.; Liu, J. J. *Am. Chem. Soc.* **2007**, *129*, 16029.
26. Xiong, H. M. *J. Mater. Chem.* **2010**, *20*, 4251.
27. Maensiri, S.; Laokul, P.; Promarak, V. *J. Cryst. Growth* **2006**, *289*, 102.
28. Pacholski, C.; Kornowski, A.; Weller, H. *Angew. Chemie. Int. Ed.* **2002**, *41*, 1188.
29. Shepherd, W. E. B.; Platt, A. D.; Hofer, D.; Ostroverkhova, O.; Loth, M.; Anthony, J. E. *Appl. Phys. Lett.* **2010**, *97*, 163303.
30. Handke, M.; Handke, B.; Kowalewska, A.; Jastrzębski, W. *J. Mol. Struct.* **2009**, *924-926*, 254.
31. Choi, S. S.; Lee, A. S.; Lee, H. S.; Jeon, H. Y.; Baek, K. Y.; Choi, D. H.; Hwang, S. S. *J. Polym. Sci. Part A: Polym. Chem.* **2011**, *49*, 5012.
32. Jeeju, P. P.; Jayalekshmi, S. *J. Appl. Polym. Sci.* **2012**, *120*, 1361.
33. Cui, F.; Liang, S.; Zhang, J.; Han, Y.; Lü, C.; Cui, T.; Yang, B. *Polym. Chem.* **2012**, *3*, 3296.
34. Liu, B.; Liu, Q.; Tong, C.; Lü, X.; Lü, C. *Colloids Surf. A* **2013**, *434*, 213.
35. Devendra, K.; Rangaswamy, T. *Mech. Confab.* **2013**, *2*, 39.
36. Huang, R.; Xu, X.; Lee, S.; Zhang, Y.; Kim, B. J.; Wu, Q. *Materials* **2013**, *6*, 4122.
37. Yamashina, N.; Isobe, T.; Ando, S. *J. Photopolym. Sci. Technol.* **2012**, *25*, 385.
38. DeSarkar, M.; Senthilkumar, P.; Franklin, S.; Chatterjee, G. J. *J. Appl. Polym. Sci.* **2012**, *124*, 215.
39. Zhang, X.; Hu, L.; Sun, D. *Acta Mater.* **2006**, *54*, 5469.
40. Gao, H.; Yorifuji, D.; Wakita, J.; Jiang, Z.-H.; Ando, S. *Polymer* **2010**, *51*, 3173.